

Time-derivative Lorentz materials and their utilization as electromagnetic absorbers

Richard W. Ziolkowski*

Electromagnetics Laboratory, Department of Electrical and Computer Engineering, The University of Arizona, Tucson, Arizona 85721

(Received 6 November 1996; revised manuscript received 12 February 1997)

A time-derivative Lorentz material model is introduced for the polarization and magnetization fields in a complex medium illuminated by an ultrafast pulsed beam. This model represents a straightforward generalization of the standard Lorentz material model to include the time derivatives of the fields as driving mechanisms. The Green function for this material is derived and used to demonstrate that it is causal and passive. An electromagnetic absorber is constructed with this time-derivative Lorentz material, and simulations are given which illustrate its effectiveness under illumination by obliquely incident, ultrafast, pulsed Gaussian beams having narrow and broad waists. [S1063-651X(97)06206-5]

PACS number(s): 41.20.Jb, 41.20.Bt

I. INTRODUCTION

Electromagnetic absorbers have many practical uses and demand for them is increasing. These include the now famous stealth technologies and practical EMI-EMC (EMI=electromagnetic interference and EMC=electromagnetic compatibility) countermeasures for personnel communications and computers, as well as the more traditional cone absorbing materials for anechoic chambers. The immense interest in complex media such as artificial chiral materials [1–4] has arisen from such needs. The artificial chiral materials such as the helix-loaded substrates [3] are worthy of particular note since they represent a very nice example of our current ability to engineer absorbers which have strong magnetic, as well as electric, properties designed into them. In contrast, artificial dielectrics have been known for many years [5–7] and have found uses, for example, as lightweight lenses and currently as photonic band gaps [8].

Absorbers have also attracted much attention recently in the computational electromagnetics community. The need to truncate the simulation domain in any finite difference or finite element approach is well known. Many approaches have been developed to achieve this truncation; they are generally classified now simply as absorbing boundary conditions (ABCs). As with any real-life absorber, the perfect ABC would absorb perfectly any frequency of electromagnetic radiation incident upon it from any angle of incidence. The Berenger perfectly matched layer (PML) ABC [9] comes quite close to this goal. In particular, the PML ABC has been shown [10–18] to be orders of magnitude more absorbing than the previously popular Mür second-order ABC [19]. However, the PML ABC is implemented in a non-Maxwellian fashion through the field equation splitting introduced by Berenger [9]. This is not a serious drawback numerically, but it does mean that a PML region cannot be realized physically.

A broad bandwidth absorbing material that is Maxwellian and hence potentially realizable with a proper engineering of artificial materials has been introduced in [20]. It is based

upon a generalization of the Lorentz model for the polarization and magnetization fields that includes the time derivative of the driving fields as a source term. The physical basis for this time-derivative Lorentz material (TD-LM) model is developed in Secs. II and III. The Green function for the TD-LM model is derived; it is used to demonstrate that the TD-LM is causal and passively absorbing. An electromagnetic absorber is constructed with this TD-LM model, and simulations are given in Sec. IV which illustrate its effectiveness under illumination by obliquely incident, ultrafast, pulsed Gaussian beams having narrow and broad waists. Analogies between the constitutive relations corresponding to the TD-LM model and those associated with bianisotropic materials are discussed in Sec. V.

II. PERFECT ABSORBER

We wish to consider the interaction of a general three-dimensional electromagnetic plane wave [$\exp(-i\omega t)$ convention assumed throughout], which is generated in free space ($z < 0$), with a semi-infinite medium ($z \geq 0$) whose normal is assumed to be in the z direction. Let the interface between these two regions be the plane $z=0$. The general obliquely incident three-dimensional plane wave case can be reduced to two orthogonal TE and TM plane wave problems [21]. For the material regions to be considered here, it is noted that the second problem could be obtained from the first one by duality. Consider then an incident plane wave which is directed from the free space region upon the interface of this semi-infinite region at the angle θ with respect to the interface's normal. This means the incident plane wave has the wave number components

$$k_x^{\text{inc}} = k_0 \sin \theta, \quad (1a)$$

$$k_z^{\text{inc}} = k_0 \cos \theta, \quad (1b)$$

which satisfy the free space dispersion relation $k_x^2 + k_z^2 = \omega^2 \epsilon_0 \mu_0$. Let the plane of incidence be spanned with the coordinates x and z . This incident two-dimensional plane wave can be either TE (perpendicular polarization or s wave) with components E_y , H_x , and H_z , or TM (parallel polarization or p wave) with components H_y , E_x , and E_z .

*FAX: (520) 621-8076. Electronic address: ziolkowski@ece.arizona.edu

If the medium ($z > 0$) is assumed to be biaxial with permittivity and permeability tensors in the frequency domain of the form

$$\frac{\bar{\epsilon}(\omega)}{\epsilon_0} = \begin{pmatrix} a_\omega & 0 & 0 \\ 0 & b_\omega & 0 \\ 0 & 0 & c_\omega \end{pmatrix}, \quad (2a)$$

$$\frac{\bar{\mu}(\omega)}{\mu_0} = \begin{pmatrix} \alpha_\omega & 0 & 0 \\ 0 & \beta_\omega & 0 \\ 0 & 0 & \gamma_\omega \end{pmatrix}, \quad (2b)$$

the separability of the TE and TM polarizations will be maintained for the transmitted field. For plane waves the Maxwell curl equations in this medium take the form $\vec{k} \times \vec{H} = -\omega \bar{\epsilon}(\omega) \cdot \vec{E}$ and $\vec{k} \times \vec{E} = +\omega \bar{\mu}(\omega) \cdot \vec{H}$. The corresponding dispersion relations for the transmitted TM and TE polarized fields in this material are immediately obtained and can be written, respectively, in the forms

$$\frac{(k_x^{\text{trans}})^2}{\beta_\omega c_\omega} + \frac{(k_z^{\text{trans}})^2}{a_\omega \beta_\omega} = \omega^2 \epsilon_0 \mu_0 = k_0^2, \quad (3a)$$

$$\frac{(k_x^{\text{trans}})^2}{b_\omega \gamma_\omega} + \frac{(k_z^{\text{trans}})^2}{\alpha_\omega b_\omega} = \omega^2 \epsilon_0 \mu_0 = k_0^2. \quad (3b)$$

The associated transmitted wave number components for the TM polarized field are

$$k_x^{\text{trans}} = k_0 \sqrt{\beta_\omega c_\omega} \sin \theta_{\text{trans}}, \quad (4a)$$

$$k_z^{\text{trans}} = k_0 \sqrt{a_\omega \beta_\omega} \cos \theta_{\text{trans}}, \quad (4b)$$

and for the TE field are

$$k_x^{\text{trans}} = k_0 \sqrt{b_\omega \gamma_\omega} \sin \theta_{\text{trans}}, \quad (5a)$$

$$k_z^{\text{trans}} = k_0 \sqrt{\alpha_\omega b_\omega} \cos \theta_{\text{trans}}. \quad (5b)$$

The corresponding transmitted electric field components for the TM polarized case are

$$E_x^{\text{trans}} + \eta_0 H_y^{\text{inc}} \left(\frac{\beta_\omega}{a_\omega} \right)^{1/2} \cos \theta_{\text{trans}}, \quad (6a)$$

$$E_z^{\text{trans}} = -\eta_0 H_y^{\text{inc}} \left(\frac{\beta_\omega}{c_\omega} \right)^{1/2} \sin \theta_{\text{trans}}, \quad (6b)$$

and for the TE polarized case are

$$H_x^{\text{trans}} = -\frac{1}{\eta_0} E_y^{\text{inc}} \left(\frac{b_\omega}{\alpha_\omega} \right)^{1/2} \cos \theta_{\text{trans}}, \quad (7a)$$

$$H_z^{\text{trans}} = +\frac{1}{\eta_0} E_y^{\text{inc}} \left(\frac{b_\omega}{\gamma_\omega} \right)^{1/2} \sin \theta_{\text{trans}}, \quad (7b)$$

where the free space wave impedance $\eta_0 = (\mu_0 / \epsilon_0)^{1/2}$. Thus the transmitted angle and the corresponding transverse wave impedance of the TM polarized case are simply

$$\theta_{\text{trans}}(\omega) = \sin^{-1}(\sin \theta / \sqrt{\beta_\omega c_\omega}), \quad (8a)$$

$$Z_{\text{trans}}(\omega) = +\eta_0 \left(\frac{\beta_\omega}{a_\omega} \right)^{1/2} \cos \theta_{\text{trans}}(\omega), \quad (8b)$$

and for the TE polarized wave case

$$\theta_{\text{trans}}(\omega) = \sin^{-1}(\sin \theta / \sqrt{b_\omega \gamma_\omega}), \quad (9a)$$

$$Z_{\text{trans}}(\omega) = -\frac{1}{\eta_0} \left(\frac{\alpha_\omega}{b_\omega} \right)^{1/2} \sec \theta_{\text{trans}}(\omega). \quad (9b)$$

Therefore the reflection coefficient for the TM polarization case is

$$R(\theta) = -\frac{1 - \sqrt{\beta_\omega / a_\omega} [\cos \theta_{\text{trans}} / \cos \theta]}{1 + \sqrt{\beta_\omega / a_\omega} [\cos \theta_{\text{trans}} / \cos \theta]} \quad (10a)$$

and for the TE polarization case is

$$R(\theta) = \frac{1 - \sqrt{b_\omega / \alpha_\omega} [\cos \theta_{\text{trans}} / \cos \theta]}{1 + \sqrt{b_\omega / \alpha_\omega} [\cos \theta_{\text{trans}} / \cos \theta]}. \quad (10b)$$

We observe that there will be no reflected wave in the TM polarization case if $\beta_\omega = a_\omega$ and $\theta_{\text{trans}} = \theta$, which from Eq. (8a) is satisfied if $\beta_\omega c_\omega = 1$. Similarly, there will be no reflected wave in the TE polarization case if $b_\omega = \alpha_\omega$ and $\theta_{\text{trans}} = \theta$, which from Eq. (9a) is satisfied if $b_\omega \gamma_\omega = 1$. In addition, if it is desired to have the TE and TM transmitted waves propagate at the same speeds (to have the same dispersion surfaces), then one must simply require $a_\omega = \alpha_\omega$. Therefore, in summary, the medium will be reflectionless for either polarization and for any angle of incidence and for any frequency if it is uniaxial and has the relative permittivity and permeability tensors of the form

$$\frac{\bar{\epsilon}(\omega)}{\epsilon_0} = \frac{\bar{\mu}(\omega)}{\mu_0} = \begin{pmatrix} a_\omega & 0 & 0 \\ 0 & a_\omega & 0 \\ 0 & 0 & 1/a_\omega \end{pmatrix} = \bar{\Lambda}_z(\omega). \quad (11)$$

The material will then be a perfect absorber if in addition

$$\text{Im}(a_\omega) > 0, \quad (12)$$

since the uniaxial medium specified by Eq. (11) produces

$$\theta_{\text{trans}} = \theta, \quad (13a)$$

$$k_x^{\text{trans}} = k_x^{\text{inc}}, \quad (13b)$$

$$k_z^{\text{trans}} = a_\omega k_z^{\text{inc}}, \quad (13c)$$

so that the transmitted wave propagates in the medium with the same angle as the incident plane wave, but with a lossy propagation constant perpendicular to the interface, i.e.,

$$\begin{aligned} \exp(i\vec{k} \cdot \vec{r}) &= \exp(ik_x^{\text{inc}} x) \exp[i \text{Re}(a_\omega) k_z^{\text{inc}} z] \\ &\quad \times \exp[-\text{Im}(a_\omega) k_z^{\text{inc}} z]. \end{aligned} \quad (14)$$

The larger the imaginary component of a_ω is, the faster the absorption in the material with respect to depth of penetration will be.

It is to be noted that the choice of the z direction for the normal to the interface was arbitrary. A reflectionless medium is achieved for any choice of the normal if the relative permittivity and permeability tensors are equal and diagonal, and if the transverse material coefficients of those tensors are equal and their longitudinal components are inverse to their transverse components. This equality of the relative permittivity and permeability tensors is unusual, but it can be motivated on physical grounds. For a dispersionless, homogeneous, isotropic medium with permittivity ϵ and permeability μ , one finds that the wave impedance in the medium matches that of free space if the ratio of the relative permeability and permittivity is one; i.e., $\sqrt{\mu/\epsilon} = \sqrt{\mu_0/\epsilon_0}$ if $\epsilon/\epsilon_0 = \mu/\mu_0$. Equation (11) is a generalization of this condition. It is also noted that it is straightforward to show that if two reflectionless media satisfying Eq. (11), one whose normal is along \underline{z} with $\underline{\Lambda}_z(\omega)$ and one whose normal is along x with $\underline{\Lambda}_x(\omega)$, intersect at right angles, then the region of intersection is reflectionless if the relative permittivity and permeability tensor in that region $\underline{\Lambda}_{xz}(\omega) = \underline{\Lambda}_x(\omega) \times \underline{\Lambda}_z(\omega)$. Similarly, if three such regions intersect at right angles, then the region of intersection is reflectionless if the relative permittivity and permeability tensor in that region $\underline{\Lambda}_{xyz}(\omega) = \underline{\Lambda}_x(\omega) \times \underline{\Lambda}_y(\omega) \times \underline{\Lambda}_z(\omega)$. If one now labels a_ω in Eq. (11) as $a_z(\omega)$ and $a_x(\omega)$ as the corresponding term in $\underline{\Lambda}_x(\omega)$ and $a_y(\omega)$ in $\underline{\Lambda}_y(\omega)$, the resulting diagonal elements of $\underline{\Lambda}_{xyz}(\omega)$ are cyclic permutations of its xx element $a_y(\omega)a_z(\omega)/a_x(\omega)$.

As argued in [21], the permittivity and permeability components a_ω and c_ω can be constructed from the corresponding frequency-domain electric and magnetic susceptibilities χ_ω so that, respectively, $a_\omega = 1 + \chi_\omega$ and $c_\omega = (1 + \chi_\omega)^{-1} = 1 - \chi_\omega(1 + \chi_\omega)^{-1}$. This means the effective electric and magnetic susceptibility tensors will be

$$\frac{\bar{\epsilon}(\omega) - \bar{1}}{\epsilon_0} = \frac{\bar{\mu}(\omega) - \bar{1}}{\mu_0} = \begin{pmatrix} \chi_\omega & 0 & 0 \\ 0 & \chi_\omega & 0 \\ 0 & 0 & -\chi_\omega/(1 + \chi_\omega) \end{pmatrix}. \quad (15)$$

Then to construct an absorber that deals effectively with ultrafast pulses, one needs to introduce a model for the susceptibility χ_ω that has a large bandwidth. As found in [20], such a susceptibility model can be developed if the polarization (magnetization) of the medium is driven with contributions from time derivatives of the electric (magnetic) fields. We note that our medium has already been assumed to have like electric and magnetic properties. As discussed by Buckingham and Dunn and Raab and co-workers [22–26], field time-derivative contributions to the polarization and magnetization fields can occur in a linear medium when it has both electric and magnetic properties. These time-derivative behaviors begin to play a nontrivial role in the ultrafast pulse regime. A similar model has been introduced in [27], a study of ultrafast light pulse interactions with resonant absorbing

media, to model more exactly the frequency dependence of the absorption coefficient far from the resonance frequency.

To model such behavior in a macroscopic sense, one can introduce a generalization of the Lorentz model for the polarization and magnetization fields that includes the time derivative of the driving fields as a driving term. For instance, the x -directed polarization field in such a material would be assumed to satisfy a linear time-derivative Lorentz material model of the form

$$\frac{\partial^2}{\partial t^2} P_x + \Gamma \frac{\partial}{\partial t} P_x + \omega_0^2 P_x = \epsilon_0 \omega_p^2 \left(\chi_\alpha E_x + \frac{\chi_\beta}{\omega_p} \frac{\partial}{\partial t} E_x \right), \quad (16)$$

where ω_0 is the resonance frequency and Γ is the width of that resonance. The terms χ_α and χ_β represent, respectively, the coupling of the electric field and its time derivative to the local charge motion. The term ω_p can be viewed as the plasma frequency associated with those charges. This TD-LM model leads to the following frequency-domain electric susceptibility:

$$\begin{aligned} \chi_\omega^{\text{TD}} &\equiv \frac{P_{\omega,x}(\vec{r})}{\epsilon_0 E_{\omega,x}(\vec{r})} = \frac{\omega_p^2 [\chi_\alpha - i(\omega/\omega_p)\chi_\beta]}{\omega_0^2 - \omega^2 - i\Gamma\omega} \\ &= \frac{(\omega_0^2 - \omega^2)\omega_p^2\chi_\alpha + \omega_p\omega^2\Gamma\chi_\beta}{(\omega_0^2 - \omega^2)^2 + (\omega\Gamma)^2} \\ &\quad + i \frac{\omega\Gamma\omega_p^2\chi_\alpha - (\omega_0^2 - \omega^2)\omega_p\omega\chi_\beta}{(\omega_0^2 - \omega^2)^2 + (\omega\Gamma)^2}. \end{aligned} \quad (17)$$

In comparison to the Lorentz model, this TD-LM model contains four independent quantities ($\omega_p^2\chi_\alpha, \omega_p\chi_\beta, \omega_0, \Gamma$) which can be adjusted to produce any desired response. The introduction of the plasma frequency in the driving terms allows the coefficients χ_α and χ_β to be dimensionless and permits a relative frequency measure between the plasma and resonance frequencies.

Choosing $\chi_\omega = \chi_\omega^{\text{TD}}$, one can satisfy Eq. (12) to make the uniaxial medium defined by Eq. (15) a passive absorber if $\text{Im}(\chi_\omega = \chi_\omega^{\text{TD}}) > 0$. From Eq. (17) this occurs if

$$\chi_\alpha > \left(\frac{\omega_0^2}{\Gamma\omega_p} \right) \left[1 - \left(\frac{\omega}{\omega_0} \right)^2 \right] \chi_\beta. \quad (18)$$

With $\chi_\alpha, \chi_\beta > 0$, this condition is satisfied for all frequencies above the resonance, i.e., for $\omega > \omega_0$. On the other hand, if, for instance, $\chi_\beta < 0$ and $\chi_\alpha > 0$, it is satisfied at all frequencies below the resonance, i.e., for $\omega_0 > \omega$. Thus, to absorb completely a given pulse (i.e., without reflections), the material must be designed to have its resonance frequency outside of the frequency spectrum of the pulse. This could be achieved in several ways. One could design the material so that $\omega_0 \sim 0$ and deal only with realistic propagating signals which would have no dc components. On the other hand, one could design materials with multiple resonances with their material constants chosen in such a manner that any pulse is completely absorbed. Nonetheless, a single resonance model would be adequate for most numerical or practical applications which would deal with pulses having band-limited frequency spectra.

Thus a broad bandwidth absorber is realized if the uniaxial TD-LM is designed so that $\chi_\alpha, \chi_\beta > 0$ and $\omega \gg \omega_0$. This results in the susceptibility

$$\chi_\omega \cong \frac{\omega_p^2 \chi_\alpha - i \omega \omega_p \chi_\beta}{-\omega^2 - i \omega \Gamma}. \quad (19)$$

If, in addition, $\omega \gg \Gamma$, the susceptibility further reduces to the form

$$\chi_\omega \cong - \left(\frac{\omega_p}{\omega} \right)^2 \chi_\alpha + i \frac{\omega_p \chi_\beta}{\omega}. \quad (20)$$

This limit would occur naturally for high frequency cases. On the other hand, if $\omega \ll \Gamma$, the susceptibility takes the form

$$\chi_\omega \cong + \frac{\omega_p}{\Gamma} \chi_\beta + i \frac{\omega_p^2}{\Gamma \omega} \chi_\alpha. \quad (21)$$

This latter case would occur when the resonance and signal frequencies are close to zero, but the resonance itself is broad.

A unit amplitude plane wave propagating along the z axis in a material, for instance, described by Eq. (20) will have the form

$$\begin{aligned} \exp(ik_z z) &= \exp[i(1 + \chi_\omega)(\omega/c)z] \\ &= \exp\{i[1 - (\omega_p/\omega)^2 \chi_\alpha](\omega/c)z\} \\ &\quad \times \exp[-(\omega_p \chi_\beta)z/c]. \end{aligned} \quad (22)$$

Clearly, such a medium will be very lossy if $\omega_p \chi_\beta \gg \omega$ in the frequency regime of interest. It will also be effectively dispersionless if in addition $\chi_\alpha \ll 1$ or $\omega_p^2 \chi_\alpha \ll \omega^2$.

III. PHYSICAL BASIS FOR THE TD-LM ABSORBER

A. Derivation of the causal TD-LM Green function

To understand the physical nature of the TD-LM model, we develop the causal Green function and general solution of Eq. (16). This time-domain equation can be written in generalized function form

$$\{\delta'' + \Gamma \delta' + \omega_0^2 \delta\} * P = \epsilon_0 [\omega_p^2 \chi_\alpha \delta + \omega_p \chi_\beta \delta'] * E, \quad (23)$$

which indicates that the corresponding Green function equation is

$$\{\delta'' + \Gamma \delta' + \omega_0^2 \delta\} * G_{\text{TD-LM}} = \epsilon_0 [\omega_p^2 \chi_\alpha \delta + \omega_p \chi_\beta \delta']. \quad (24)$$

Hence the requisite impulse response is

$$G_{\text{TD-LM}} = \epsilon_0 \{\delta'' + \Gamma \delta' + \omega_0^2 \delta\}^{-1} [\omega_p^2 \chi_\alpha \delta + \omega_p \chi_\beta \delta']. \quad (25)$$

We proceed with the knowledge of the standard Lorentz model's Green function problem:

$$\{\delta'' + \Gamma \delta' + \omega_0^2 \delta\} * G_L = \delta, \quad (26)$$

which has the well-known causal solution

$$\begin{aligned} G_L(t) &= \{\delta'' + \Gamma \delta' + \omega_0^2 \delta\}^{-1} \\ &= \exp\left(-\frac{\Gamma t}{2}\right) \frac{\sin \omega t}{\omega} Y(t) \equiv g_L(t) Y(t), \end{aligned} \quad (27)$$

where $Y(t)$ is the Heaviside function and

$$\omega = \sqrt{\omega_0^2 - \Gamma^2/4}. \quad (28)$$

Thus one finds that the Green function to Eq. (16) is

$$\begin{aligned} G_{\text{TD-LM}}(t) &= \epsilon_0 [\omega_p^2 \chi_\alpha \delta + \omega_p \chi_\beta \delta'] * G_L(t) \\ &= \epsilon_0 \omega_p^2 \chi_\alpha G_L(t) + \epsilon_0 \omega_p \chi_\beta \delta' G_L(t) \\ &= \epsilon_0 \exp\left(-\frac{\Gamma t}{2}\right) Y(t) \left\{ \omega_p^2 \chi_\alpha \frac{\sin \omega t}{\omega} + \epsilon_0 \chi_\beta \frac{\omega_p}{\omega} \right. \\ &\quad \left. \times \left[-\frac{\Gamma}{2} \sin(\omega t) + \omega \cos(\omega t) \right] \right\}. \end{aligned} \quad (29)$$

Introducing the terms

$$\cos(\omega t_R) = \frac{\Gamma}{2\omega_0}, \quad (30a)$$

$$\sin(\omega t_R) = \frac{\omega}{\omega_0}, \quad (30b)$$

$$\chi_R = \chi_\beta \frac{\omega_0}{\omega_p} \exp\left(-\frac{\Gamma t_R}{2}\right), \quad (30c)$$

the expression (29) for the TD-LM Green function becomes

$$\begin{aligned} G_{\text{TD-LM}}(t) &= \epsilon_0 \omega_p^2 \exp\left(-\frac{\Gamma t}{2}\right) Y(t) \left[\chi_\alpha \frac{\sin(\omega t)}{\omega} \right. \\ &\quad \left. - \chi_\beta \frac{\omega_0}{\omega_p} \frac{\sin[\omega(t-t_R)]}{\omega} \right] \\ &= \epsilon_0 \omega_p^2 [\chi_\alpha g_L(t) - \chi_R g_L(t-t_R)] Y(t). \end{aligned} \quad (31)$$

Since the solution to Eq. (16) is simply $P(t) = G_{\text{TD-LM}}(t) * E_x(t)$, this result shows that the TD-LM model involves two ordinary Lorentz-type dipole terms, one shifted in time from the other by a real valued constant time shift t_R . We note that Eq. (31) immediately demonstrates that the TD-LM Green function is causal [the presence of the Heaviside function $Y(t)$] and passive (the presence of the exponential decay term in g_L). According to the explanation given in [28], p. 309, the passive nature of the TD-LM model (16) is also expressed by the result that

$$G_{\text{TD-LM}}(0_+) = \epsilon_0 \omega_p \omega_0 \chi_\beta \frac{\sin(\omega t_R)}{\omega} \equiv \epsilon_0 \omega_p \chi_\beta > 0. \quad (32)$$

This conclusion coupled with Eq. (22) also shows that the χ_β terms are to be associated with the loss mechanisms in the TD-LM model. From Eq. (31) this means that these loss mechanisms are associated with an out-of-phase oscillator component which results from the time derivatives of the electric field in Eq. (16).

B. Plausibility arguments for the field time derivative in the TD-LM

To uncover a naturally occurring or an artificially constructed material exhibiting the TD-LM behavior, one must understand further the possible physical origins of the time-derivative behavior in Eq. (16). The presence of the field time derivative in the TD-LM model can be further motivated from microscopic arguments dealing with two-level atom media. It has been shown by Ziolkowski, Arnold, and Gogny [29] at this quantum mechanical level that such a time-derivative field behavior exists and can contribute significantly to the behavior of materials when ultrafast pulses are interacting with it. If one examines the first-order Maxwell-Bloch equations describing electromagnetic wave interaction with a two-level atom medium and the resulting second-order system, one finds that the instantaneous responses of the dispersive and quadrature terms are, respectively, $\rho_1 \sim \omega_0^{-2} (2\gamma/\hbar) \rho_3 E$ and $\rho_2 \sim \omega_0^{-2} (2\gamma/\hbar) \rho_3 \partial_t E$, where γ is the dipole coupling coefficient and ρ_3 is a measure of the population difference between the ground and the excited state [$\rho_3 = -1 (+1)$ occurs when all of the atoms are in the ground (excited) state]. This means that the retarded responses of the system will be governed to first order by the damped spring oscillator equations

$$\begin{aligned} \partial_t^2 \rho_1 + \frac{1}{T_2} \partial_t \rho_1 + \omega_0^2 \rho_1 &= -\frac{\omega_0}{T_2} \rho_2 + \frac{2\gamma}{\hbar} \rho_3 \omega_0 E \\ &\sim \rho_3 \frac{2\gamma}{\hbar T_2} \left((\omega_0 T_2) E - \frac{1}{\omega_0} \partial_t E \right), \end{aligned} \quad (33a)$$

$$\begin{aligned} \partial_t^2 \rho_2 + \frac{1}{T_2} \partial_t \rho_2 + \omega_0^2 \rho_2 &= +\frac{\omega_0}{T_2} \rho_1 + \frac{2\gamma}{\hbar} \rho_3 \omega_0 \partial_t E \\ &\sim \rho_3 \frac{2\gamma}{\hbar T_2} [E + T_2 \partial_t E]. \end{aligned} \quad (33b)$$

The appearance of the time derivative of the electric field in Eq. (33a) is associated with the loss terms which are characterized by the dephasing time T_2 of the system. Since the polarization $P = -N_{\text{atom}} \gamma \rho_1$ of this medium, where N_{atom} is the number of two-level atoms per unit volume in it, the appearance of the TD-LM model is immediate.

A time derivative of the electric (magnetic) field also appears in the polarization (magnetization) expression obtained by time-dependent perturbation expansion analysis in nonrelativistic quantum mechanics. Following the development given by Buckingham and Dunn [22], let the medium be a set of atoms described by the Hamiltonian $\hat{H} = \hat{H}_0 + \hat{H}_{\text{int}}$, where \hat{H}_0 describes the unperturbed part and \hat{H}_{int} represents the interaction part resulting from the electromagnetic field. The unperturbed wave functions of the system $\Psi_n^{(0)} = \psi_n^{(0)} \exp(-i\omega_n t)$ satisfy the Schrödinger equation $\hat{H}_0 \Psi_m^{(0)} = \hbar \omega_m \Psi_m^{(0)}$. The quantum mechanical state of the perturbed medium can then be described by the wave function $\Psi(\vec{r}, t) = \sum_m c_m(t) \psi_m^{(0)} e^{-i\omega_m t}$ if the time-dependent coefficients $c_m(t)$ are obtained. From time-dependent analysis these coefficients are given by the expressions $c_m(t)$

$-c_m(0) = (i\hbar)^{-1} \sum_k \int_0^t dt' H_{mk}^{(1)}(t') c_k(t') e^{-i\omega_m t'}$, where the frequency differences $\omega_{mk} = \omega_m - \omega_k$ and the transition matrix coefficients $H_{mk}^{(1)} = \langle m | \hat{H}_{\text{int}} | k \rangle$. The usual procedure is to assume that the medium is prepared in a single quantum state of the unperturbed Hamiltonian, i.e., $c_k(0) = \delta_{kn}$ and the system then evolves by the presence of the perturbing interaction term. The resulting perturbation expression for the time-dependent coefficients is

$$c_m(t) \approx \frac{1}{i\hbar} \int_0^t dt' H_{mn}^{(1)}(t') e^{-i\omega_{mn} t'}. \quad (34)$$

Let the perturbing electric field be causal. [$\vec{E}(t) = 0$ for $t < 0$ and $\vec{E}(t) \neq 0$ for $t > 0$] and have the form $\vec{E}(t) = \vec{E}_0 \sin \omega t$ for $t \geq 0$. The interaction Hamiltonian is given by the expression $H_{\text{int}}(t) = -\vec{p} \cdot \vec{E}(t)$, where \vec{p} is the electric dipole moments of the atom. The dipole matrix coefficients are given by the expression $\vec{d}_{ij} = \langle i | \vec{p} | j \rangle$. Relaxation losses are introduced with the substitution $\omega_{mn} \rightarrow \omega_{mn} - i\Gamma_{mn}/2$, $\Gamma_{mn} \ll \omega_{mn}$ being the width of the transition. The coefficients (29) of the perturbed wave function then have the values

$$\begin{aligned} c_m(t) \approx \frac{i}{\hbar} \left\{ \vec{d}_{mn} \cdot [i\omega_{mn} \vec{E}(t) - \partial_t \vec{E}(t)] \times \frac{\exp(-i\omega_{mn} t)}{\omega^2 - \omega_{mn}^2 + i\Gamma_{mn}} \right\} \\ + C_e, \end{aligned} \quad (35)$$

where C_e is a time-independent constant which depends on the initial values of the electric field and its time derivative. Note that the single frequency (ω) excitation electric field and its time derivative have been reintroduced explicitly in this expression to emphasize the appearance of those terms. Similar arguments lead to analogous expressions for the magnetic field and magnetic dipole terms.

The polarization vector of this linear medium, assuming again that it is composed of N_{atom} atoms per unit volume, is then obtained immediately from the observable

$$\begin{aligned} \vec{P}(t) &= N_{\text{atom}} \sum_{m,n} \langle m | \vec{p} | n \rangle \\ &= 2 \text{Re} \sum_{m,n} \vec{d}_{mn} c_{mn}^*(t) e^{-i\omega_{mn} t} \approx \bar{\alpha}_0 \cdot \vec{E} + \bar{\alpha}_1 \cdot \partial_t \vec{E}. \end{aligned} \quad (36)$$

In comparison, well below the resonance frequency where the perturbation analysis would be appropriate, the time derivatives of the polarization in Eq. (16) are negligible and Eq. (16) reduces to the approximate form

$$P_x \approx \epsilon_0 \left(\frac{\omega_p}{\omega_0} \right)^2 \left(\chi_\alpha E_x + \frac{\chi_\beta}{\omega_p} \frac{\partial}{\partial t} E_x \right). \quad (16')$$

Thus in agreement with Eq. (16') the polarization vector (36) depends not only on the electric field, but also on its time derivative. It should be noticed that, as discussed in connection with Eq. (16), the time-derivative term in Eq. (36) is most naturally associated with the imaginary part of the transition matrix, hence with the loss of mechanisms.

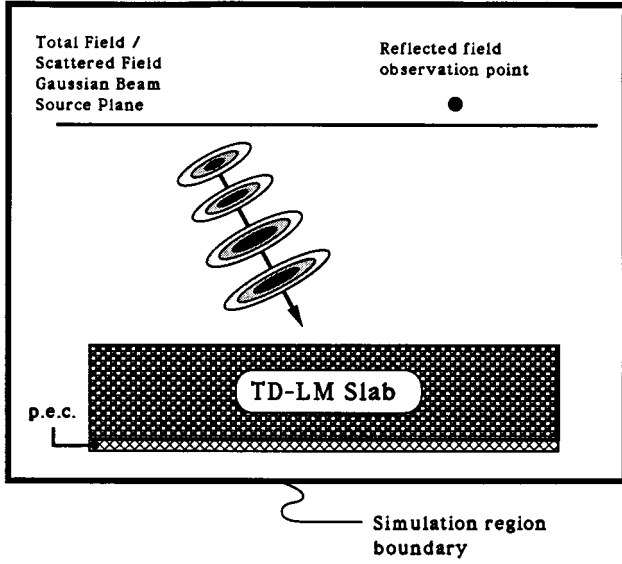


FIG. 1. The absorption properties of a perfect electric conductor-backed TD-LM slab are characterized by measuring the reflected field arising when it is illuminated by a pulsed Gaussian beam.

IV. TD-LM ABSORBER NUMERICAL SIMULATION

The effectiveness of a broad bandwidth, dispersionless TD-LM absorber is illustrated with the TM Gaussian beam scattering geometry shown in Fig. 1. The absorber is taken to be a thin slab ($\lambda/5$ at the center frequency of the beam) that is terminated away from the source with a perfect electric conductor. The reflection from the termination enhances the absorption in the medium since the reflected wave also passes through the absorber. Thus the scatterer is a metallic sheet coated with a thin film of the absorber. This scattering process is modeled with the finite-difference time-domain (FDTD) simulator described in Ref. [20]. A reflectionless uniaxial Maxwellian material with the susceptibilities

$$\chi_{xx}^E(\omega) = \frac{P_x}{\epsilon_0 E_x} = \frac{\omega_p^2 [\chi_\alpha - i(\omega/\omega_p)\chi_\beta]}{\omega_0^2 - \omega^2 - i\Gamma\omega}, \quad (37a)$$

$$\chi_{yy}^M(\omega) = \frac{M_y}{H_y} = \frac{\omega_p^2 [\chi_\alpha - i(\omega/\omega_p)\chi_\beta]}{\omega_0^2 - \omega^2 - i\Gamma\omega}, \quad (37b)$$

$$\chi_{zz}^E(\omega) = \frac{P_z}{\epsilon_0 E_z} = -\frac{\omega_p^2 [\chi_\alpha - i(\omega/\omega_p)\chi_\beta]}{[\omega_0^2 + \omega_p^2 \chi_\alpha] - \omega^2 - i[\Gamma + \omega_p \chi_\beta]\omega} \quad (37c)$$

is included in the FDTD simulator by solving Maxwell's curl equations

$$\frac{\partial}{\partial t} \vec{E} = \frac{1}{\epsilon_0} \nabla \times \vec{H} - \frac{1}{\epsilon_0} \frac{\partial}{\partial t} \vec{P}, \quad (38a)$$

$$\frac{\partial}{\partial t} \vec{H} = -\frac{1}{\mu_0} \nabla \times \vec{E} - \frac{\partial}{\partial t} \vec{M} \quad (38b)$$

self-consistently with the corresponding time-domain polarization and magnetization equations:

$$\frac{\partial^2}{\partial t^2} P_x + \Gamma \frac{\partial}{\partial t} P_x + \omega_0^2 P_x = \epsilon_0 \omega_p^2 \left[\chi_\alpha E_x + \frac{\chi_\beta}{\omega_p} \frac{\partial}{\partial t} E_x \right], \quad (39a)$$

$$\frac{\partial^2}{\partial t^2} M_y + \Gamma \frac{\partial}{\partial t} M_y + \omega_0^2 M_y = \omega_p^2 \left[\chi_\alpha H_y + \frac{\chi_\beta}{\omega_p} \frac{\partial}{\partial t} H_y \right], \quad (39b)$$

$$\begin{aligned} \frac{\partial^2}{\partial t^2} P_z + [\Gamma + \omega_p \chi_\beta] \frac{\partial}{\partial t} P_z + [\omega_0^2 + \omega_p^2 \chi_\alpha] P_z \\ = -\epsilon_0 \omega_p^2 \left[\chi_\alpha E_z + \frac{\chi_\beta}{\omega_p} \frac{\partial}{\partial t} E_z \right]. \end{aligned} \quad (39c)$$

Note that the perfect reflectionless Maxwellian material behaves as a TD-LM in the directions parallel to the interface and as a TD-LM with a wider resonance whose location is shifted in the directions perpendicular to the interface. If the coefficients satisfy Eq. (18), this medium will be a perfect (passive) absorber. It is to be noted that the presence of the explicit negative sign in the driving functions in Eq. (37c) and hence Eq. (39c) might be interpreted as necessitating the medium to have gain in the longitudinal direction. This is not the case. It must be emphasized that the Green function corresponding to Eq. (39c), which has the same form as Eq. (26), is also exponentially decaying and therefore no gain is realized. Nonetheless, the question of how to achieve this sign reversal for the longitudinal component in a real or an artificial material is currently under investigation.

An ultrafast pulsed TM Gaussian beam [30,31] is launched with either a waist of 2λ or 200λ from a position on the indicated source plane (numerically we generate a Gaussian beam at the source plane with Huygens' principle and propagate the beam from the source plane towards the slab in a total field region and measure the reflected beam in the scattered field region away from the source plane) that will produce a beam whose center coincides with the center of the interface of this slab. For illustration purposes only, the frequency of the beam was chosen to be 2.0×10^{13} Hz. The pulse was a six-cycle sinusoid tapered on its first and last two cycles with a smooth function. The beam is polarized in the x - z plane. The TD-LM parameters were chosen to be $\omega_0 = \omega_p = 2\pi \times 2.0 \times 10^{13}$, $\Gamma = 1.0 \times 10^5$, $\chi_\alpha = 1.0 \times 10^{-10}$, and $\chi_\beta = 2.2 \times 10^6$. The material parameters in the FDTD TD-LM slab are given a quadratic profile to minimize numerical reflections from the slab-air interface [20]. The amplitude reflection coefficient from the slab was obtained in the scattered field region by measuring the maximum in time of H_y^{refl} at a point along the central ray of the reflected beam, scaling it by the amplitude transport coefficient of the beam (which accounts for the amplitude decay in distance from the source), and normalizing the result with respect to the corresponding value of H_y^{inc} at the interface. These amplitude reflection coefficients for the narrow and wide beam cases are plotted in Fig. 2 as a function of the angle of incidence of the Gaussian beam on the slab. The corresponding plane wave and line source results are given in Ref. [20]. Significant absorption of both beams was realized even with a thin

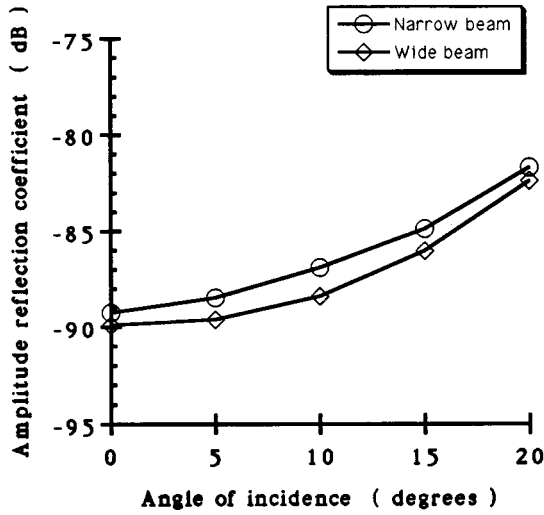


FIG. 2. The amplitude reflection coefficients for narrow and wide pulsed Gaussian beams show the perfect electric conductor-backed TD-LM slab to be an excellent absorber.

TD-LM layer. These pulsed Gaussian beam results indicate that the absorber is handling well both wideband spatial and temporal frequencies.

V. COMMENTS

The TD-LM model leads to constitutive relations of the form [20]

$$\vec{D} = \bar{\epsilon} \cdot \vec{E} + \bar{\Gamma}^E \cdot \partial_t \vec{E} = \bar{\epsilon} \cdot \vec{E} + \bar{\gamma}^E \cdot \nabla \times \vec{B}, \quad (40a)$$

$$\vec{H} = \bar{\mu}^{-1} \cdot \vec{B} + \bar{\Gamma}^B \cdot \partial_t \vec{B} = \bar{\mu}^{-1} \cdot \vec{B} + \bar{\gamma}^B \cdot \nabla \times \vec{E}, \quad (40b)$$

which are similar to those encountered in Refs. [22–26] and are analogous to the Drude-Born-Fedorov model associated with bianisotropic media such as optically active and chiral materials [1–4]:

$$\vec{D} = \bar{\epsilon} \cdot \vec{E} + \bar{\Gamma}^E \cdot \partial_t \vec{B} = \bar{\epsilon} \cdot \vec{E} + \bar{\gamma}^E \cdot \nabla \times \vec{E}, \quad (41a)$$

$$\vec{H} = \bar{\mu}^{-1} \cdot \vec{B} + \bar{\Gamma}^B \cdot \partial_t \vec{E} = \bar{\mu}^{-1} \cdot \vec{B} + \bar{\gamma}^B \cdot \nabla \times \vec{B}. \quad (41b)$$

The difference between these constitutive relations resides in the exchange of \vec{E} and \vec{B} in the curl terms. Nonetheless, they are rather similar in form. Moreover, artificial chiral materials have been constructed and tested experimentally [2,3]. These observations have led to the suggestions made in [20]

for realizing a slab of the TD-LM absorber using specifically designed electromagnetic scatterers (loaded antennas) embedded in a matrix to achieve an artificial electric and magnetic material with the requisite polarization and magnetization characteristics. The properties of these small loaded antennas can be adjusted to obtain those characteristics. However, as pointed out by Roberts [32,33], there are many equivalent ways to realize a particular dispersive medium. Thus more effective realizations might be achievable. Several potential constructions of an artificial TD-LM are now being actively considered.

VI. CONCLUSIONS

In this paper physical justifications of the time-derivative Lorentz material model were described and discussed. It was shown that an ideal absorber could be constructed with a uniaxial, dispersive and lossy, electric and magnetic region specified by a model which was introduced for both the polarization and the magnetization fields. With a Green function solution to the TD-LM polarization (magnetization) equation it was demonstrated that the TD-LM was causal, passive, and was constructed from two ordinary Lorentz-type dipole terms, one shifted in time from the other by a real valued time constant. This analysis also emphasized the connections between the terms proportional to the time derivatives of the fields and the TD-LM loss mechanisms. The numerical implementation of a TD-LM slab terminated with perfect electric conductor was discussed, and numerical tests of this configuration were defined. The numerical tests demonstrated the effectiveness of the TD-LM slab in absorbing broad bandwidth pulsed Gaussian beams having narrow and broad beam waists.

ACKNOWLEDGMENTS

The author would like to thank John Cloete, University of Stellenbosch, for many enjoyable discussions about complex artificially designed materials, their classifications, and the novel effects resulting from their realizations. The author would also like to thank Tom Roberts of the USAF Rome Laboratory for his suggestions which led to the Green function analysis of the TD-LM model and Peter Petropoulos of the Applied Mathematics Department at SMU for making Ref. [27] known to me during the revision process so it could be included here. This work was sponsored in part by the Office of Naval Research under Grant No. N0014-95-1-0636 and by the Air Force Office of Scientific Research, Air Force Material Command, USAF, under Grant Number F49620-96-1-0039.

- [1] I. V. Lindell, A. H. Sihvola, S. A. Tretyakov, and A. J. Vitantonen, *Electromagnetic Waves in Chiral and Bi-isotropic Media* (Artech, Boston, 1994), pp. 8–14.
 [2] F. Mariotte, S. A. Tretyakov, and B. Sauviac, *IEEE Microwave Opt. Tech. Lett.* **7**, 861 (1994).
 [3] *Proceedings Chiral'94 Workshop*, 3rd International Workshop on Chiral, Bi-isotropic and Bi-anisotropic Media, Pergueux France, May 18–20, 1994, edited by F. Mariotte and J.-P.

- Parneix (C.E.A/C.E.S.T.A., Le Barp, France, 1994).
 [4] R. E. Raab and J. H. Cloete, *J. Electromagn. Waves Appl.* **8**, 1073 (1994).
 [5] J. Brown, in *Progress in Dielectrics*, edited by J. B. Birks and J. H. Schulman (Heywood, London, 1960), Vol. 2, pp. 194–225.
 [6] M. M. Z. Kharadly and W. Jackson, *Proc. IEEE (London)* **100**, 199 (1953).

- [7] Z. A. Kaprielian, *J. Appl. Phys.* **27**, 24 (1956).
- [8] J. D. Joannopoulos, R. D. Meade, and J. N. Winn, *Photonic Crystals* (Princeton University Press, Princeton, NJ, 1995).
- [9] J.-P. Berenger, *J. Comput. Phys.* **114**, 185 (1994).
- [10] D. S. Katz, E. T. Thiele, and A. Taflove, *IEEE Microwave Guided Wave Lett.* **4**, 268 (1994).
- [11] W. C. Chew and W. H. Weedon, *IEEE Microwave Opt. Tech. Lett.* **7**, 599 (1994).
- [12] C. E. Reuter, R. M. Joseph, E. T. Thiele, D. S. Katz, and A. Taflove, *IEEE Microwave Guided Wave Lett.* **4**, 344 (1994).
- [13] C. M. Rappaport, *IEEE Microwave Guided Wave Lett.* **5**, 90 (1995).
- [14] R. Mittra and Ü Pekel, *IEEE Microwave Guided Wave Lett.* **5**, 84 (1995).
- [15] W. V. Andrew, C. A. Balanis, and P. A. Tirkas, *IEEE Microwave Guided Wave Lett.* **5**, 192 (1995).
- [16] D. C. Wittwer and R. W. Ziolkowski, *Electromagnetics* **16**, 465 (1996).
- [17] L. Zhao and A. C. Cangellaris, *IEEE Microwave Guided Wave Lett.* **6**, 209 (1996).
- [18] Z. S. Sacks, D. M. Kingsland, R. Lee, and J.-F. Lee, *IEEE Trans. Antennas Propag.* **AP-43**, 1460 (1995).
- [19] G. Mür, *IEEE Trans. Electromagn. Compat.* **EMC-23**, 377 (1981).
- [20] R. W. Ziolkowski, *IEEE Trans. Antennas Propag.* **45**, 656 (1997).
- [21] J. Kong, *Electromagnetic Waves* (Wiley, New York, 1986), pp. 110 and 111.
- [22] A. D. Buckingham and M. B. Dunn, *J. Chem. Soc. A* 1988 (1971).
- [23] E. B. Graham and R. E. Raab, *Proc. R. Soc. London* **430**, 593 (1990).
- [24] E. B. Graham and R. E. Raab, *Philos. Mag. B* **64**, 267 (1991).
- [25] D. A. Imrie and R. E. Raab, *Mol. Phys.* **74**, 833 (1991).
- [26] E. B. Graham and R. E. Raab, *J. Appl. Phys.* **69**, 2549 (1991).
- [27] V. A. Vasilev, M. Ya. Kelbert, I. A. Sazonov, and I. A. Chaban, *Opt. Spektrosk.* **64**, 862 (1988) [*Opt. Spectrosc. (USSR)* **64**, 513 (1988)].
- [28] J. D. Jackson, *Classical Electrodynamics*, 2nd ed. (Wiley, New York, 1975), p. 309.
- [29] R. W. Ziolkowski, J. A. Arnold, and D. M. Gogny, *Phys. Rev. A* **52**, 3082 (1995).
- [30] R. W. Ziolkowski and J. B. Judkins, *J. Opt. Soc. Am. A* **9**, 2021 (1992).
- [31] J. B. Judkins and R. W. Ziolkowski, *J. Opt. Soc. Am. A* **12**, 1974 (1995).
- [32] T. M. Roberts, in *Invariant Imbedding and Inverse Problems*, Proceedings of the Symposium on Invariant Imbedding and Inverse Problems, edited by James P. Coronas (SIAM, Philadelphia, 1992), Chap. 9.
- [33] T. M. Roberts, in *Second International Conference on the Mathematical and Numerical Aspects of Wave Propagation*, edited by R. Kleinman, T. Angell, D. Colton, F. Santosa, and I. Stakgold (SIAM, Philadelphia, 1993), Chap. 44.